Proceedings of the 6th International Caribbean Conference on Devices, Circuits and Systems, Mexico, Apr. 26-28, 2006

Leakage Current Analysis of a Real World Silicon-Silicon Dioxide Capacitance

P. Schwaha, R. Heinzl, T. Grasser, CDL–IUE TU Wien, Gußhausstraße 27–29, A–1040 Vienna, Austria
W. Brezna, J. Smoliner, FKE TU Wien, Floragasse 7, A–1040 Vienna, Austria
H. Enichlmair, R. Minixhofer, austriamicrosystems AG, Schloss Premstätten, A–8141 Unterpremstätten, Austria
Email: {schwaha, heinzl, grasser}@iue.tuwien.ac.at

***Abstract*— It is shown that surface roughness becomes increasingly important as oxide thicknesses decrease. Silicon-silicon dioxide capacitances with thicknesses of 7 nm, 15 nm, and 50 nm are measured with an atomic force microscope (AFM). The height data thusly obtained is used to create three dimensional simulation structures to reproduce measurement data obtained from leakage current measurements. The leakage currents are simulated using the Fowler-Nordheim (FN) tunnelling current model.**

I. Introduction

During the investigation of gate leakage measurements of oxides with different thicknesses, as shown in Figure I, it became apparent that taking only the flatband voltage of each of the measured devices into account is insufficient for understanding the measured data. This is shown in Figure I where the tunnelling currents do not overlap with the theoretical Fowler-Nordheim (FN) curve.

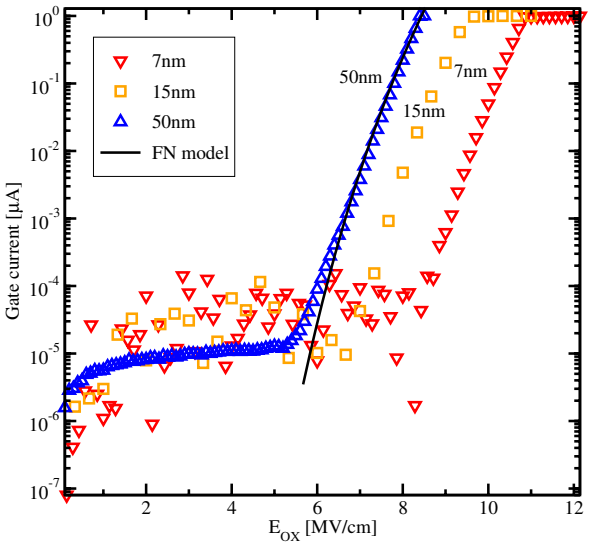

Fig. 1: Comparison of the measured oxide tunnelling currents. The measurements were performed at *austriamicrosystems*.

Although the regions indicated in the figure exhibit the characteristics of FN tunnelling the curves should overlap for this tunnelling mechanism. It was suspected that three-dimensional effects due to surface roughness are at least partially responsible for the observed discrepancy. This spawned interest on how to describe these three-dimensional effects. To investigate the influence of surface roughness on the electrical characteristics of oxides, height data sets obtained from AFM measurements were used as input parameters for modelling. The measured samples provided by *austriamicrosystems* corresponded to the ones subject to the leakage current investigation and were measured at the Institute for Solid State Electronics at the Technical University of Vienna.

II. AFM Measurements

To overcome the difficulties with raw data sets from AFM measurement a pre-processing module (AFMStructureBuilder: ASBuilder) has been developed to correct the raw data sets and to perform the three-dimensional meshing step and contact building.

A. Raw Data Sets

The raw data set from AFMs measurement are used although some post-processing steps could be done within the measurement software. This is because these steps must be done very accurately and in correlation with the following device simulation steps for a detailed investigation. ASBuilder was developed with these considerations in mind. Figure Fig. 2 shows an output of the measurement software.

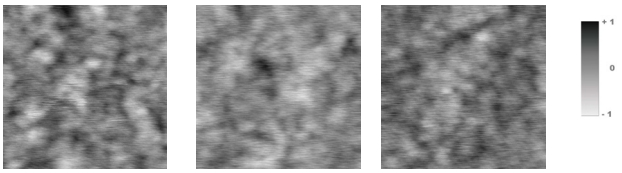

Fig. 2: Two-dimensional height distribution of the AFM measurement (left: 7 nm, middle: 15 nm, right: 50 nm).

To enhance the raw data set ASBuilder can filter the data set with different options designed to compensate for different effects encountered during the measurement[1].

- Piezo drift
  Due to heating of the AFM tip during the measurement period the piezo crystal drift results in an z-offset of the measured data set. Within ASBuilder this piezo drift can be recomputed and compensated.

- Fast-scan-line noise
  To reduce fast-scan-line noise a discrete Fourier filter is used to suppress this kind of noise.
- Spike filtering
  To filter noise spikes gauss filters with different kernels can be applied within ASBuilder.

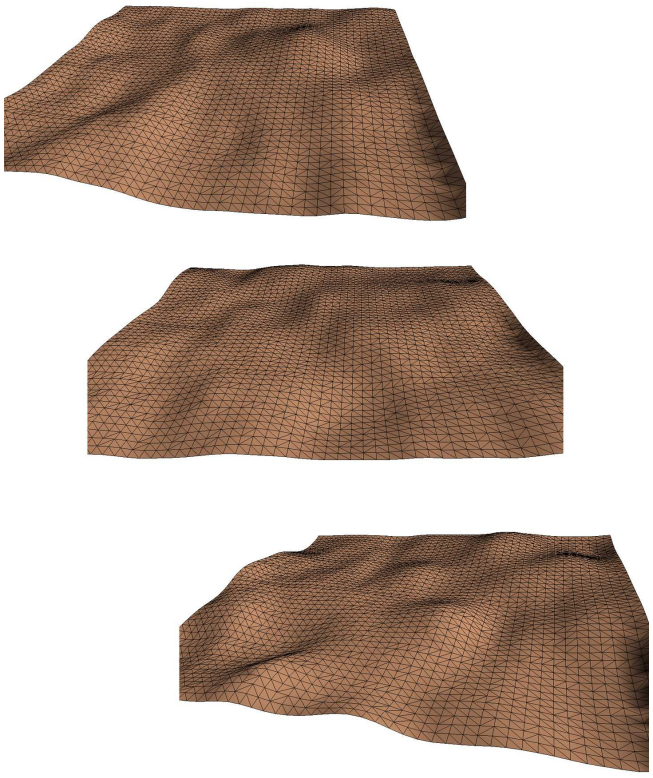

Fig. 3: A detailed view of the height distribution (top: 7 nm, middle: 15 nm, bottom: 50 nm).

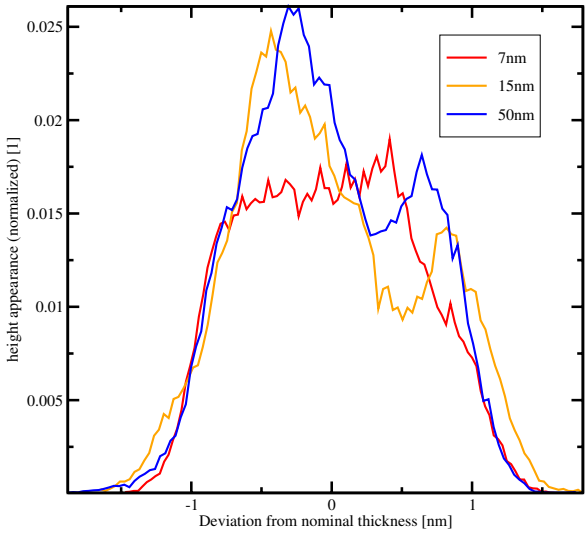

Fig. 4: Histograms of the height distributions.

C. Building the Three-Dimensional Simulation Structures

To investigate oxide reliability in detail the prepared and triangulated surfaces of the oxides are meshed by ASBuilder [2] into a three-dimensional object with a bottom and top metallic contact.

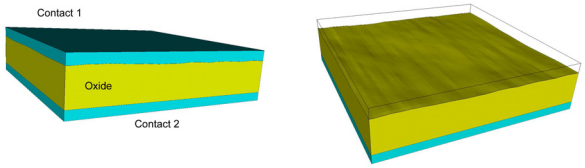

Fig. 5: Three-dimensional oxide structure.

B. Further Processing of Data Sets

For further processing ASBuilder creates a surface triangulation of the corrected and adjusted height distribution. In order to accomplish this ASBuilder reads in the height distribution data set, corrects the data set and assembles a two-dimensional height distribution matrix. From this matrix an unstructured two-dimensional mesh is generated where the data set is meshed (ASBuilder) with a so called height-map meshing step where the height distribution is triangulated and elevated into three dimensions. The result can be seen in Figure Fig. 3.

The histograms of the height distributions presented in Figure Fig. 4 show the characteristics of the three different oxides. Here the 7 nm oxide has the flattest distribution which means that the surface roughness is equally distributed between the complete range of 6 nm to 8 nm. The presumably high fluctuations of the 15 and 50 nm oxide are insignificant when compared to the overall thickness of the oxide, while the same does not hold for the 7 nm oxide.

With this pre-processing steps of ASBuilder a completely three-dimensional object with the non-planar oxide element and two planar contacts is created which can be used as input data for any existing device simulation software such as Minimos-NT [3] to calculate the electric field distribution required for the modelling of FN tunnelling.

III. Simulation Methodology

After the extensive preparations outlined above several simulation steps need to be performed. First, the electric field distribution is calculated. The results of the three-dimensional electric field calculation are shown in Figure Fig. 6 and Fig. 7. Figure Fig. 6 depicts the absolute values of the electric field, while Figure Fig. 7 shows a cut through the three-dimensional simulation domain. Both figures illustrate the influence of the encountered surface roughness on the electric field. The field clearly shows peaks in the regions of thinner oxide inducing heightened electrical stress in these regions.

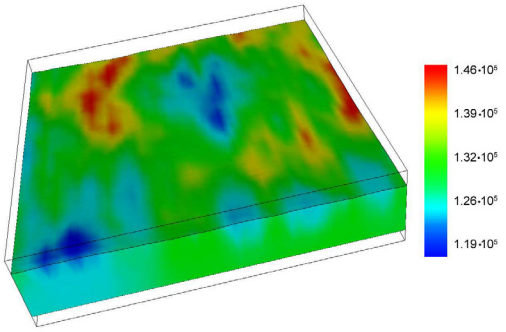

Fig. 6: Results of a three-dimensional simulation of the electric field distribution for a $50\times50\,\mathrm{nm}^2$ region of a 7 nm oxide. The values of the electric field are in V/cm.

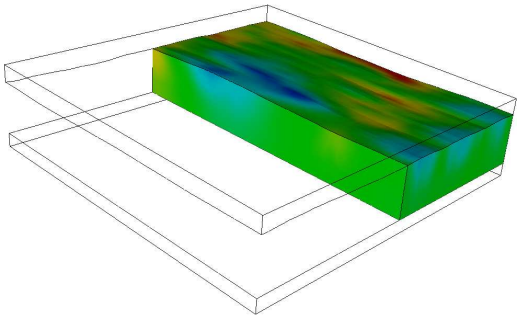

Fig. 7: Cut through the simulation domain of a $50\times50\,\mathrm{nm}^2$ region of a 7 nm oxide.

Due to the thickness of the oxides and the strong electric fields the leakage current is modelled as FN tunnelling current. It is evaluated using the previously determined electric field distribution. The FN tunnelling current is modelled by the well known expression [4], [5]

$$J = a\,|E|^2\,\exp\left(-\frac{b}{|E|}\right).$$

The parameters $a = 994.63\times10^{-9}\,\mathrm{A/V^2}$ and $b = 2.64\times10^{10}\,\mathrm{V/m}$ were calibrated for the non-planar case of each oxide thickness and then used in the subsequent simulations.

IV. Comparison of the Measured Leakage Currents

The area below the 50 nm oxide is ohmically connected to the bulk of the wafer, while the areas corresponding to the thinner oxides are insulated by pn-junctions. The measured structures are schematically presented in Figure Fig. 8 for the 50 nm oxide and in Figure Fig. 9 for the 7 and 15 nm oxides. This explains the differing noise levels visible in the measurement data (Figure I) as the measurements of the 7 and 15 nm oxides also include noise from this junction.

The measured data includes several effects that complicate the analysis. The flatband voltage is one such interference within this measurement. The pn-junctions included in the 7 and 15 nm structures contribute another parasitic effect within the measurement. Both of these effects need to be taken into account in order to enable a correct modelling of the

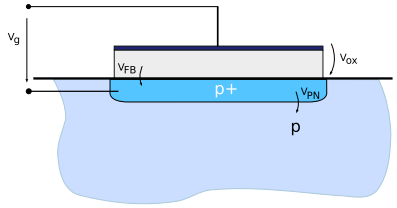

Fig. 8: Structure of measurement arrangement (50 nm).

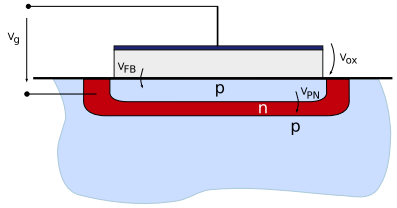

Fig. 9: Structure of measurement arrangement (7 nm and 15 nm).

leakage current. Figure Fig. 10 shows the influence of the flatband voltage. While the influence on the 50 nm oxide is marginal, there is a significant impact for the thinner oxides. The compensation of the influence of the pn-junctions on the thinner oxides is shown in Figure Fig. 11. Again the influence is larger for smaller oxide thicknesses.

$$E'_{\mathrm{ox}} = \frac{V - V_{\mathrm{pn}}}{t_{\mathrm{ox}}}$$

After amending for these effects the measurement curves almost overlap as can be observed in Figure Fig. 13. This is an indication of a common mechanism of the leakage current which is readily found in FN tunnelling.

V. Simulation Results

After considering the flatband voltage, the pn-junction voltage and the previously determined correction voltages the regions depicted in Figure I overlap, as can be seen in Figure Fig. 13, and can then be simulated with the FN tunnelling model. The result obtained from this simulation is also depicted in Figure Fig. 13. The agreement between the measured leakage current and the simulation result is excellent. Using the parameters obtained from the non-planar case, a simulation with planar surfaces is performed as well. This is done by calculating the average height of the oxide from the distribution and assuming a parallel plate capacitor. This corresponds to an effective thickness extracted from CV measurements. The results of this computation is shown in Figure Fig. 12. As expected the non-planar curves overlap. The discrepancy between the planar and non-planar case increases with decreasing oxide thickness. This indicates that the relative roughness is responsible for this deviation which, as already stated above, increases as the oxide thickness is reduced. From this it is evident that non-planar effects are increasingly important as oxide thicknesses shrink. From the comparison of the fully three-dimensional and the planar simulations correction voltages can be derived.

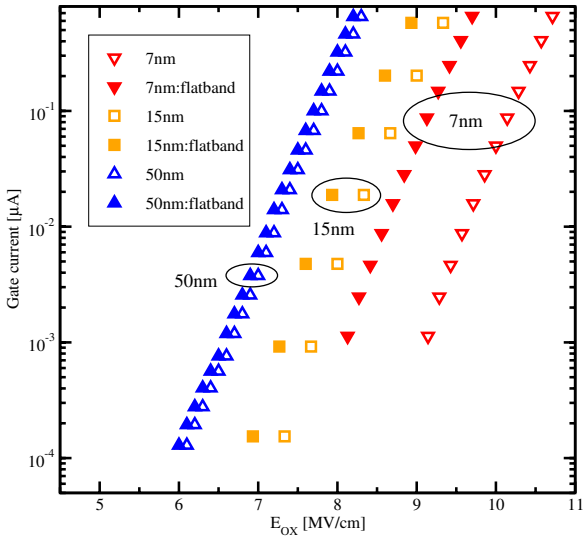

Fig. 10: Comparison of the original data set and the corrected set obtained by inclusion of the flatband voltage.

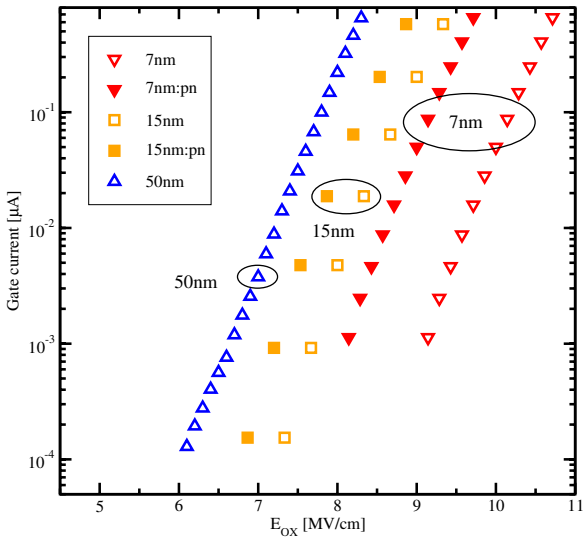

Fig. 11: Comparison of the original data set and the data corrected by the pn-junction.

The observed tunnelling current is not only important for the overall power consumption of devices but also for the reliability of the devices [4], as the tunnelling charge carriers are responsible for damaging the oxide and deteriorating the performance of the device.

VI. Conclusion

Due to the growing complexity of the structures of modern semiconductor devices and the ongoing shrinking to smaller dimensions, device simulations in two dimensions are no longer sufficient because of dominant three-dimensional effects. This is especially true for oxide properties due to the reduction of oxide thickness to only a few atomic layers.

In particular we have shown that by considering only the effective oxide thickness obtained for instance from CV measurements the estimated FN currents are significantly underestimated due to the non-planarity of the oxide. This effect increases for decreasing oxide thicknesses and has to be considered for oxide reliability considerations.

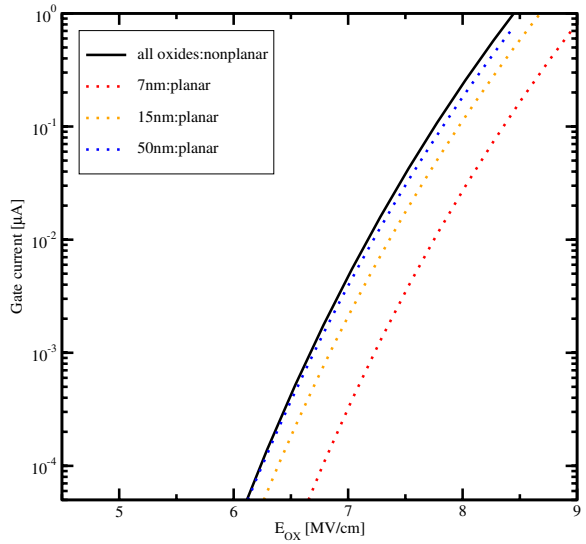

Fig. 12: Comparison of the influence of three-dimensional surface roughness effects.

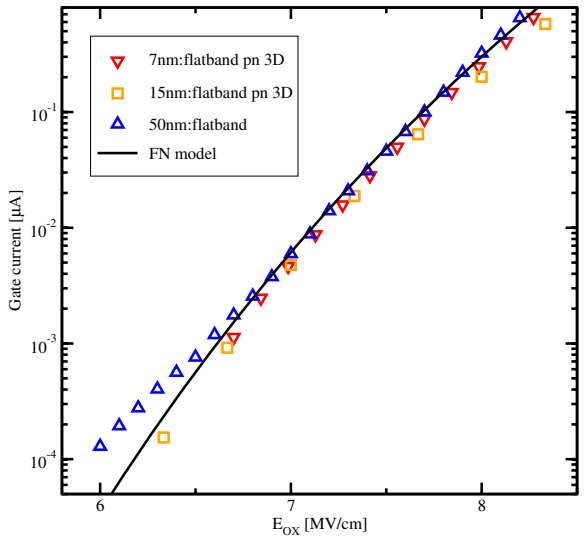

Fig. 13: Final simulation compared to corrected measurement data sets.

References

[1] C. Chao-Jung, Dissertation, Technische Universität Ilmenau, 2003.
[2] P. Fleischmann and S. Selberherr, in *Proc. SISPAD* (Kobe, Japan, 2002), pp. 99–102.
[3] IμE, *MINIMOS-NT 2.1 User's Guide*, Institut für Mikroelektronik, Technische Universität Wien, Austria, 2005, http://www.iue.tuwien.ac.at/software/minimos-nt.

[4] A. Ghetti, in *Predictive Simulation of Semiconductor Processing*, edited by E. W. J. Dabrowski (Springer, 2004), pp. 201–258.
[5] M. Lenzlinger and E. H. Snow, J.Appl.Phys. **40**, 278 (1969).